Fine structure in the α decay of ^{188,192}Po

K. Van de Vel,[1] A. N. Andreyev,[2,*] D. Ackermann,[3,4] H. J. Boardman,[2] P. Cagarda,[3] J. Gerl,[3] F. P. Heßberger,[3] S. Hofmann,[3] M. Huyse,[1] D. Karlgren,[1,5] I. Kojouharov,[3] M. Leino,[6] B. Lommel,[3] G. Münzenberg,[3] C. Moore,[2] R. D. Page,[2] S. Saro,[3] P. Van Duppen,[1] and R. Wyss[5]

[1]*Instituut voor Kern- en Stralingsfysica, University of Leuven, Celestijnenlaan 200D, 3001 Leuven, Belgium*
[2]*Oliver Lodge Laboratory, University of Liverpool, Liverpool L69 7ZE, United Kingdom*
[3]*Gesellschaft für Schwerionenforschung, Planckstrasse 1, 64291 Darmstadt, Germany*
[4]*Johannes Gutenberg-Universität, 55099 Mainz, Germany*
[5]*Department of Physics, Royal Institute of Technology, 104 05 Stockholm, Sweden*
[6]*Department of Physics, University of Jyväskylä, 40014 Jyväskylä, Finland*

(Received 3 July 2003; published 21 November 2003)

The α decay of ^{188,192}Po has been reexamined in order to probe the 0^+ states in the daughter nuclei ^{184,188}Pb that can be associated with coexisting spherical, oblate, and/or prolate configurations. Improved values were measured for the excitation energy and the feeding α-decay intensity of the 0^+_2 state in ^{184,188}Pb and conflicting results on the 0^+_3 state in ^{188}Pb were clarified. All known cases of fine structure in the α decay of the even-even Po nuclei are reviewed. The reduced α-decay width systematics combined with potential-energy-surface calculations confirm the onset of deformation in the ground state of the polonium nuclei around the neutron midshell. An isomeric state with a half-life of 580(100)ns has been identified in ^{192}Po.

DOI: 10.1103/PhysRevC.68.054311 PACS number(s): 23.20.Lv, 23.20.Nx, 23.60.+e, 27.70.+q

I. INTRODUCTION

Shape coexistence at low excitation energy in neutron-deficient polonium and lead nuclei is a well-established phenomenon studied extensively both from theoretical (see, e.g., Refs. [1–3] and references therein) and experimental (see, e.g., Refs. [4–7] and references therein) points of view. While the spherical shape is attributed to the $Z=82$ shell closure, the deformed configurations are associated with intruder states resulting from the excitation of one or more proton pairs across the $Z=82$ shell gap. For example, for lead nuclei, the oblate π(two particle-two hole) and prolate $\pi(4p\text{-}4h$ or $6p\text{-}6h)$ configurations coexist with the spherical $\pi(0p\text{-}0h)$ configuration. As it is difficult to observe excited 0^+ states in heavy-ion induced fusion-evaporation reactions using γ-ray spectroscopy, we use the fine structure in the α decay to study the excited 0^+ states [8]. One of the best studied cases to date is the neutron midshell nucleus ^{186}Pb in which a low-lying prolate deformed band was observed in in-beam studies [9,10]. In an α-decay study of ^{190}Po two excited 0^+ states were populated in ^{186}Pb [5]; a special feature in this case is that both of these states lie below the first excited 2^+ state. While the ground state of ^{186}Pb is associated with the spherical configuration, the excited 0^+ states mainly comprised the oblate and prolate configurations. The substantial α-decay feeding of the excited 0^+ states in ^{186}Pb is made possible by an admixture of the deformed configuration in the ground-state wave function of ^{190}Pb [11].

In this work we investigated shape coexistence for the even-even neighbors (^{188}Pb and ^{184}Pb) of ^{186}Pb through fine structure in the α decay of ^{192}Po and ^{188}Po, respectively. Although the α decay of ^{188,192}Po has been studied before [4,12–15], the present study is well motivated.

The isotope ^{188}Po was identified recently [12] and fine-structure decay to an excited 0^+ state in ^{184}Pb was observed. However, due to the low production cross section only a few events were observed. This resulted in a large uncertainty for the half-life ($T_{1/2}=400^{+200}_{-150}$ μs) and for the intensities of the 7915(25)-keV[I_α=65(20)%] and the 7350-keV[I_α=35(20)%] transitions attributed to this nucleus.

In ^{188}Pb an excited 0^+_2 state has been observed in various α-decay studies of ^{192}Po [4,13–15] and in an in-beam conversion electron experiment [16]. There is a large variation in the values for the excitation energy of the 0^+_2 state and for the feeding α-decay intensity although most values are consistent within the errors as can be seen from Table I. Some features that are representative of the quality of the data, such as the reaction channel used to produce ^{192}Po and the statistics obtained, are also listed.

A candidate for a second excited 0^+ state in ^{188}Pb was identified in only two studies: one at 767(12)keV, populated via α decay [14], and one at 725(2)keV by observing in-beam conversion electron transitions [16]. In ^{188}Pb the levels of the yrast band with $I^\pi>2^+$ have been associated with a prolate configuration [9]. Recently a collective nonyrast band presumably of oblate character has been observed, the interband γ-ray transitions to the prolate yrast band indicate mixing between the oblate and prolate configurations [17].

In the present experiment we aimed to determine more precise values for the excitation energies of the excited 0^+ states in ^{184,188}Pb as well as for the intensity of the feeding α decay. This is necessary to extract accurate reduced α-decay width values which provide via α-decay mixing calculations detailed insight into nuclear shapes and underlying shell structures as discussed in Ref. [8].

II. EXPERIMENTAL SETUP

The experiment was performed at the velocity filter SHIP at GSI, Darmstadt. The detection setup was identical to that

*Corresponding author. Email address: aan@ns.ph.liv.ac.uk

TABLE I. Details of the various fine-structure α-decay studies of ^{192}Po and of the in-beam conversion electron study of ^{188}Pb. Indicated are the excitation energy of the first excited 0_2^+ state, the number of counts in the ground-state to ground-state $^{192}\text{Po}\rightarrow{}^{188}\text{Pb}$ decay, the ratio of the α-decay intensity to the first excited and lowest 0^+ states, and the reaction channel.

$E(0_2^+)$ (keV)	$I_\alpha(0_1^+)$	$I_\alpha(0_2^+)/I_\alpha(0_1^+)$	Reaction	References
571(31)	450[a]	$1.0(4)\times10^{-2}$	^{160}Dy(^{36}Ar, 4*n*)^{192}Po	[13]
568(4)	1.2×10^{4}[b]	$1.47(19)\times10^{-2}$	^{160}Dy(^{36}Ar, 4*n*)^{192}Po	[14]
591(10)	1.1×10^{3}[a]	$1.9(7)\times10^{-2}$	^{160}Dy(^{36}Ar, 4*n*)^{192}Po and ^{164}Er(^{32}S, 4*n*) ^{192}Po	[4,15]
591(2)			^{156}Gd(^{36}Ar, 4*n*)^{188}Pb	[16]
588(4)	1.6×10^{5}[a]	$1.5(3)\times10^{-2}$	^{142}Nd(^{52}Cr, 2*n*)^{192}Po	This work

[a]Number of single α particles, both beam on and beam off. In this work the number of α particles during the beam off periods is 1.2×10^5.
[b]Number of correlated α particles, $\Delta T(\text{recoil-}\alpha)\leqslant 200$ ms. This gives a ratio $\alpha(^{192}\text{Po})/\alpha(\text{total})=6.75\%$ [14] to be compared with $\alpha(^{192}\text{Po})/\alpha(\text{total})=80\%$ in the present work with a correlation time of 90 ms.

described in Ref. [12] where a complete overview was provided, so experimental details are only summarized here. The complete fusion reaction ^{142}Nd(^{52}Cr, 2*n*)^{192}Po at a beam energy of 4.25 MeV/nucleon (in the middle of the target) was used to produce ^{192}Po. The ^{188}Po nuclei were produced in the ^{142}Nd(^{50}Cr, 4*n*)^{188}Po reaction at a beam energy of 5.04 MeV/nucleon (in the middle of the target). The ^{142}Nd targets (isotopic enrichment of 99.8%) with a thickness of 290 μg/cm^2 were evaporated as $^{142}Nd_2F_3$ material onto carbon layers of 50 μg/cm^2 thickness and covered with a 10-μg/cm^2 layer of carbon. The ^{52,50}Cr ions were delivered by the UNILAC heavy ion accelerator with a pulsing rate of 5 ms on/15 ms off and an intensity of about 200 pnA. Recoiling reaction products were separated using the velocity filter SHIP [18,19] and then implanted into a 300-μm-thick position sensitive silicon detector (PSSD). The detector consisted of 16 strips of 5×35 mm^2 in size, each position sensitive in the vertical direction with a position resolution of 400 μm. For the recoils and their subsequent α decays, the position, energy, and time of detection were recorded.

In front of the PSSD six silicon detectors of the same shape were arranged in an open box geometry. These were used to detect conversion electrons from the prompt decay of the excited states populated by the α decay. One fourfold segmented Clover detector was placed as close as possible behind the PSSD in order to detect α-γ coincidences and γ rays emitted in the decay of isomeric states. The absolute efficiency determination of the electron and Clover detectors followed the method detailed in Ref. [12].

III. EXPERIMENTAL RESULTS

A. α decay of ^{192}Po

Figure 1(a) shows the α-particle energy spectrum for the ^{52}Cr+^{142}Nd reaction at a beam energy of 4.25 MeV/nucleon (in the middle of the target) collected between beam pulses. The peak at 7167(4) keV corresponds to the known ground-state to ground-state α decay of ^{192}Po. Due to a factor of 10 higher statistics compared to previous studies a more precise value for the half-life of 31.8(15)ms could be measured. From $\alpha_1(^{192}\text{Po}, 7167\text{ keV})$-$\alpha_2(^{188}\text{Pb}, 5980\text{ keV})$ correlations an α-decay branching ratio of 8.0(6)% was deduced for ^{188}Pb, in agreement with the values of 8.5(13)% [13] and 9.3(8)% [15]. Other polonium and bismuth isotopes were produced including ^{193}Po with a decay energy E_α =7004 keV and a half-life $T_{1/2}$=240 ms for the 13/2$^+$ isomer; the 3/2$^-$ isomer has a decay energy E_α=6949 keV and a half-life $T_{1/2}$=450 ms [20]. The energy spectrum for α particles shown in Fig. 1(b) was generated in an identical matter to that of Fig. 1(a), but demanding that the α particles are detected within 90 ms of the implantation of a recoil in the same PSSD position. The contribution from the heavier

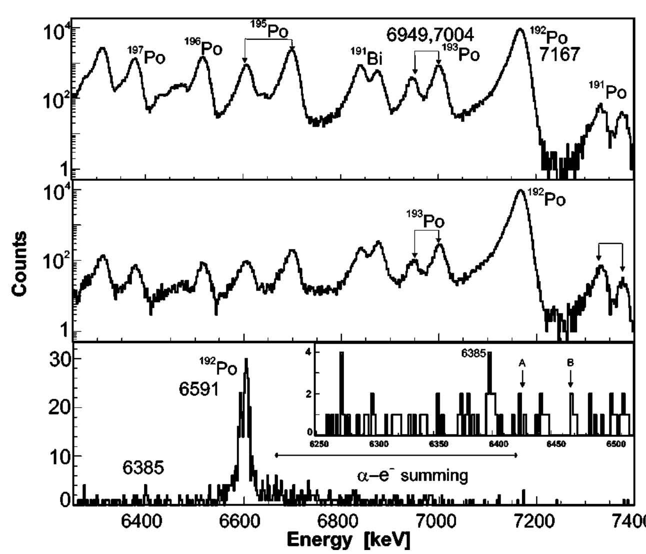

FIG. 1. (a) Single α-particle energy spectrum collected in the ^{52}Cr+^{142}Nd reaction between the beam pulses. The prominent peaks are assigned to known activities and for some specific lines the α-particle energies are given in keV. (b) Energy spectrum of α decays correlated with a recoil within 90 ms. (c) The same spectrum as in (b), but in prompt coincidence with a low-energy signal registered in the electron detector. The inset shows the spectrum expanded for the energy range 6250 keV–6550 keV.

polonium and bismuth isotopes is greatly reduced owing to their longer half-lives compared to ^{192}Po.

Figure 1(c) shows the energy spectrum of α particles occurring within 90 ms of a recoil implantation adding a constraint that the α particle is in prompt coincidence with a low-energy ($<$1000 keV) signal registered in the electron detectors. The α peaks in this spectrum need energy and intensity corrections as the conversion electron leaves part of its energy in the PSSD when it escapes towards the electron detectors. This electron energy sums up with the α-particle energy and gives rise to a shift in the centroid and to a high-energy tail of the α peak, indicated with "α-e^- summing" in Fig. 1(c). The minimum energy left by the conversion electron in the PSSD was found to be 10 keV from the energy shift of the 6431-keV α-particle decay of ^{190}Bi (which populates an excited state in ^{186}Tl) when adding the constraint that the α particle is followed by a conversion electron (^{190}Bi was produced in the ^{52}Cr+^{142}Nd reaction at a beam energy of 5.27 MeV/nucleon in the middle of the target). A detailed account of the α-electron energy summing in the PSSD, including simulations using the Monte Carlo code GEANT [21,22] is given in Ref. [12]. Applying the energy correction we obtain an energy of 6591(8) keV for the prominent line in Fig. 1(c). It correlates with the 5980 keV α decay of ^{188}Pb as its daughter and hence is attributed to fine structure in the α decay of ^{192}Po. Note that in the following we will use the α-particle energies obtained after the α-electron summing correction. No coincidences between the 6591-keV α line and γ rays, except for coincidences with Pb K x rays were observed. This fine-structure α decay is therefore interpreted as feeding a 0^+ state in ^{188}Pb at 588(4) keV (deduced from the Q_α values) which further decays by internal conversion to the ground state, confirming the results of Refs. [4,13–16]. The intensity of the high-energy tail of the 6591-keV peak amounts to 50(5)% of the intensity of the 6591 keV α line, in agreement with the GEANT calculations. This results in a total intensity [after correcting for the electron detector efficiency of 35(5)%] of 1.5(3)% for the decay to the 0^+ state at 588 keV in ^{188}Pb relative to the 7167-keV ground-state decay. Comparison with previous measurements summarized in Table I shows that the present results are in agreement with and more precise than most of them. We note that in Ref. [13] the α-electron summing effects were not taken into account in the energy and intensity determination for the fine-structure α decay which explains the lower values. This correction was included in Refs. [4,15] whose results are in a better agreement with the present data. The intensity determined for the feeding α line in Ref. [14] is consistent with our data although the energy measured for the 0_2^+ state is somewhat lower than all other results.

In Fig. 1(c) a weak peak is indicated at 6385(15) keV, as can be seen in the inset showing the spectrum expanded for the energy range 6250 keV-6550 keV. This α peak lies within the energy range of the fine-structure α decay E_α =6416(13) keV of the decay to the 767-keV 0^+ state suggested by Allatt *et al.* [14] whose position is indicated by arrow *A*. However, the reported α branching ratio of 0.75(27)% for the decay to the 767 keV state would yield about 200 α (6416 keV) events in Fig. 1(c), a value considerably higher than the number of counts observed. An alternative explanation for the 6416(13)-keV peak reported in Ref. [14] could be that it arose from fine structure in the α decay of ^{193}Po which was studied recently [23]. A $13/2^+$ state at 637(1) keV in ^{189}Pb was populated by the 6375(15)-keV α decay of the $13/2^+$ isomer of ^{193}Po. Similarly, a $13/2^-$ state at 549(1) keV in ^{189}Pb is populated by the 6420(20) -keV α decay of the $3/2^-$ isomer of ^{193}Po. Both the excited $13/2^+$ and $13/2^-$ states in ^{189}Pb further decay via converted transitions to the lowest $13/2^+$ and $13/2^-$ states, respectively. The conversion coefficient α_{tot}=1.1(4) of the 637-keV transition and the α branching ratios reported in Ref. [23] together with the intensity of the 7004-keV ground-state transition of Fig. 1(b), would give 10(4) counts at α(6375 keV) $+e^-$(10 keV)=6385 keV. Therefore we assign the peak at 6385(15) keV of Fig. 1(c) to fine structure in the α decay of ^{193}Po. We note that by taking a correlation time of 750 ms (optimized for ^{193m}Po decay with a half-life of 240 ms) the number of counts observed at α(6375 keV)$+e^-$(10 keV) =6385 keV agrees with the number of counts expected on the basis of the data of Ref. [23]. This means that there is no evidence for a 0^+ state at 767(12) keV in ^{188}Pb as was reported in Ref. [14].

Population of the 0^+ state at 725 keV identified in the recoil-gated in-beam conversion electron study by Le Coz *et al.* [16] would correspond to an α-particle energy of 6457 keV. In their study the conversion electrons from the 725-keV transition could not be placed in the level scheme through coincidence measurements, but were assumed to feed the ground state and hence established an excited 0^+ state at 725 keV. The position for a 6457-keV α line is indicated with arrow *B* in Fig. 1(c). As the number of counts in this region of Fig. 1(c) is on the background level, the present data do not provide evidence for the presence of this fine-structure α line and hence do not support the 0^+ state at 725 keV in ^{188}Pb. An upper limit of 0.3% for the α decay to this state relative to the decay to the 588-keV 0^+ state has been deduced. This gives an intensity of less than 0.005% relative to the ground-state to ground-state decay. The non-observation of a 6457-keV α line can be due to the fact that the 725-keV level is not populated in the α decay of ^{192}Po and hence has a very high hindrance factor (see Table II) or to the fact that this level does not exist. The electron line observed in Ref. [16] could also come from highly converted $J \rightarrow J$ (with $J \neq 0$) transitions expected at higher energy in the level scheme.

B. Isomeric transitions in ^{192}Po

In neutron-deficient even-mass Po isotopes isomeric states with I^π=8^+, 11^-, and 12^+ have been observed [24,25], the 11^- isomer has been found down to ^{194}Po. Figure 2 shows an energy spectrum of γ-ray spectrum deexciting an isomer. The γ rays were measured by the Clover detector at the focal plane of the SHIP within 5 μs after a recoil implantation in the PSSD which was followed by the 7167-keV α decay of ^{192}Po within 90 ms. The observed γ-ray transitions are labeled by energy and transitions that have been observed pre-

TABLE II. Overview of the fine-structure α-decay characteristics for $^{188-198}$Po. Indicated are the half-life, the energy E_α, and the α-decay branching ratio I_α of the ground state to ground-state and the fine-structure α decays, the excitation energy E_{exc} for the populated $0^+_{2,3}$ states, the reduced α-decay width δ^2, and the hindrance factor HF. For $^{194-198}$Po the half-lives, energies, and intensities of the different fine-structure lines are taken from Refs. [30–33]. The total α-decay branching ratio for ^{188,190,192}Po was taken to be 100%.

^{A}Po		E_α (keV)	I_α (%)	E_{exc} (keV)	δ^2 (keV)	HF
^{188}Po, 270(30) μs	0^+_1	7910(15)	80(4)	0	30(4)	1
	0^+_2	7355(35)	20(4)	572(30)	370(130)	0.08(3)
^{190}Po, 2.45(5) ms	0^+_1	7533(10)	96.4(4)	0	51(4)	1
	0^+_2	7012(20)	3.3(4)	533	90(18)	0.57(12)
	0^+_3	6896(20)	0.3(1)	660	21(8)	2.4(9)
^{192}Po, 31.8(15) ms	0^+_1	7167(4)	98.6(2)	0	57(2)	1
	0^+_2	6591(7)	1.4(1)	588(4)	102(22)	0.56(7)
	0^+_3	(6457)[a]	$\leqslant$0.005[b]	725(2)[c]	$\leqslant$1.14	$\geqslant$50
^{194}Po, 392(4) ms	0^+_1	6842(6)	93(7)	0	54(7)	1
	0^+_2	6194(7)	0.22(2)	658(4)	44(5)	1.2(2)
^{196}Po, 5.8(2) s	0^+_1	6521(5)	94(5)	0	55(4)	1
	0^+_2	5769(6)	$2.1(2)\times10^{-2}$	768.5(17)	21(2)	2.6(2)
^{198}Po, 105(3) s	0^+_1	6180(4)	57(2)	0	42(3)	1
	0^+_2	5273(4)	$7.6(13)\times10^{-4}$	930.6(9)	13(3)	3.2(5)

[a]Fine-structure α-particle energy deduced from the ground-state to ground-state transition energy and the excitation energy of the 0^+_3 state from Ref. [16].
[b]Only an upper limit for the intensity of this line can be given, see text.
[c]Taken from Ref. [16].

viously in in-beam γ-ray studies [24,26] are indicated with stars. The rotational-like band identified up to (10^+) in the in-beam studies is shown as an inset to Fig. 2. Owing to the lack of coincidences in the present data the new transitions

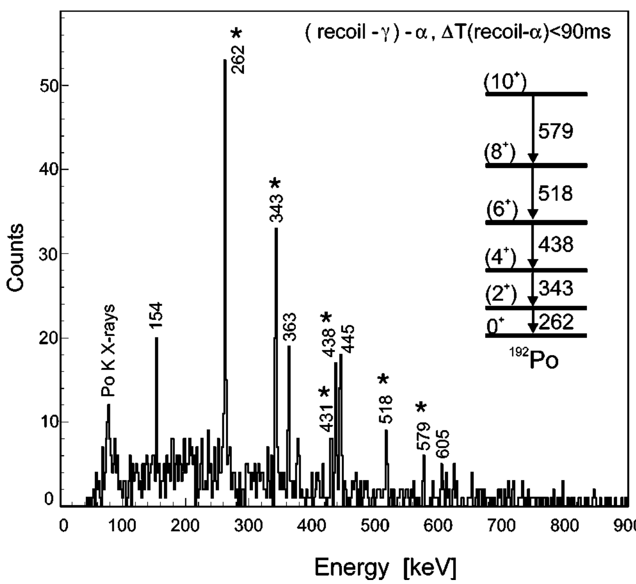

FIG. 2. Energy spectrum of γ-rays deexciting an isomer. The γ rays were measured by the focal plane Clover detector in coincidence with recoils tagged with the α decay of ^{192}Po. Energies are given in keV, the transitions labeled with stars have been observed previously via in-beam γ-ray spectroscopy studies reported in Refs. [24,26]. The inset shows the ground-state band for ^{192}Po from Refs. [24,26].

could not be placed in the existing level scheme of ^{192}Po. As the recoil-γ time distribution is similar for the different transitions, they were assumed to deexcite from the same isomer that must be situated above the (10^+) state in ^{192}Po as the (10^+) to (8^+) 579-keV transition was observed. A half-life value of 580(100) ns was extracted for this isomer in ^{192}Po. We want to draw the attention to the lowest-energy transition in Fig. 2 that occurs at 154 keV. Based on the amount of K x rays observed, an upper limit for the conversion coefficient of this transition indicates that the 154-keV transition is of $E1$ multipolarity. This may hint to the presence of an 11^- state at 2295 keV which deexcites via the 154-keV transition to the 10^+ state and via nonyrast transitions (not observed in the in-beam γ-ray studies) that feed the lower-spin levels of the yrast band.

C. α decay of ^{188}Po

By using the ^{142}Nd(^{50}Cr, $4n$)^{188}Po reaction with a beam energy of 5.04 MeV/nucleon (in the middle of the target) improved statistics were obtained confirming the initial identification of ^{188}Po α decay [E_α=7915(15) keV and $T_{1/2}$ $=400^{+200}_{-150}$ μs] discussed in Ref. [12] in which the ^{142}Nd(^{50}Cr, $6n$)^{188}Po reaction was employed with beam energies of 5.54 MeV/nucleon and 5.65 MeV/nucleon. Figure 3 shows the combined spectra from the two experiments. Figure 3(a) displays an α-particle energy spectrum produced under the condition that the α particle is preceded within 1.2 ms by a recoil in the same PSSD location. The α-decay peak at 7910(15) keV is the ground-state to ground-state α decay of ^{188}Po. Based on the higher statistics an improved half-life value of 275(30) μs was deduced. Figure 3(b) shows a two-

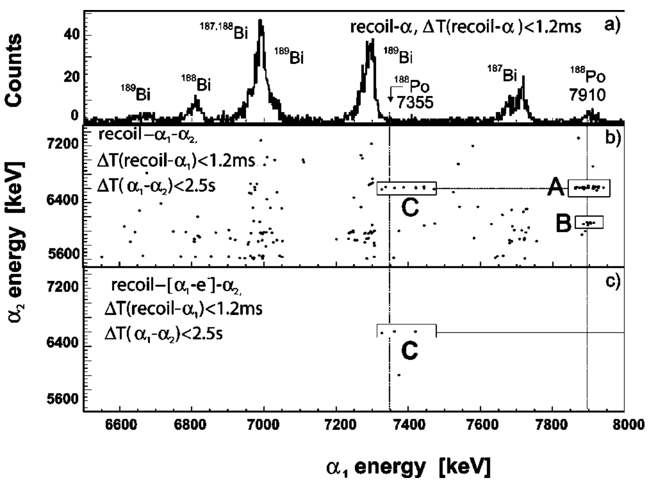

FIG. 3. (a) Energy spectrum of α decays correlated with a recoil within 1.2 ms using the ^{52}Cr+^{142}Nd and ^{50}Cr+^{142}Nd reactions. The prominent peaks are assigned to known activities and for some specific lines the α-particle energies are given in keV. (b) Mother and daughter α-particle energies for all chains of the type recoil-α_1-α_2. Maximum correlation times were 1.2 ms for the recoil-α_1 pair and 2.5 s for the α_1-α_2 pair. (c) The same as in (b), but in prompt coincidence with a signal registered in the electron detector.

dimensional α-particle energy plot of all chains of the type recoil-α_1-α_2 (α_1 and α_2 refers to the parent and daughter α decays, respectively). Correlation times were 1.2 ms for the recoil-α_1 pair and 2.5 s for the α_1-α_2 pair. A group of recoil-α_1-α_2 chains indicated by rectangle *A* was assigned to the decay chain 188Po-184Pb [$E\alpha 2$=6632(10) keV, $T1/22$=550(60) ms] [27]. From these data a value of 80(15)% was obtained for the α-decay branching ratio of ^{184}Pb. A recent proton-decay study of ^{185}Bi gave a similar α-decay branching ratio for ^{184}Pb [28]. The α-decay branching ratio value obtained in these two measurements is considerably larger than the value of 23(14)% given in Ref. [29].

The observation of the recoil-^{188}Po-^{180}Hg [E_α =6116 keV, $T_{1/2}$=2.56(2) s] decay chains indicated by rectangle *B* yields an α-decay branching ratio of 45(20)% for ^{180}Hg, in agreement with the value of 48(2)% [27].

A group of nine events [indicated by rectangle *C* in Fig. 3(b) is present at α_1=7355(35) keV and α_2=6606(20) keV, the decay properties for the daughter activity being compatible with ^{184}Pb α decay [27]. Three of these chains remain when a prompt coincidence is required between the mother α particle and an event detected in the electron detectors as shown in Fig. 3(c). We assign these events to fine-structure α decay of ^{188}Po to a 0^+ state at 572(30) keV in ^{184}Pb in agreement with Ref. [12]. Due to the low production of ^{188}Po and due to a low γ-ray detection efficiency no γ-ray coincidences were observed for ^{188}Po.

D. Results

The characteristics of the α decays of $^{188-198}$Po to the 0^+ states in $^{184-194}$Pb are summarized in Table II. The data for ^{186}Pb are taken from Ref. [5]. The energies and intensities for the fine-structure α lines of ^{194,196,198}Po are taken from Refs. [30–33]. The reduced α width δ^2 is calculated using the method of Rasmussen [34]. The hindrance factor (HF) indicates the strength of the fine-structure α decay relative to the ground-state decay, for which a HF=1 is assumed.

IV. DISCUSSION

Several theoretical approaches [1–3] have been used to describe the presence of low-lying deformed configurations (and in some cases the mixing with the spherical configuration) for lead nuclei. All calculations reproduce the general trend of the excitation energy of the oblate and/or prolate 0^+ states as a function of neutron number. However, in most calculations the absolute excitation energy is not in agreement with the experimental data and the different approaches vary in the neutron number for which the deformed configurations achieve a minimum.

In the following we combine potential-energy-surface (PES) calculations based on the Nilsson-Strutinsky approach [35] with the α-decay data to deduce information on the excited 0^+ states in ^{184,186,188}Pb and on the ground states of ^{188,190,192}Po. The PES calculations describe the evolution of the coexisting minima in polonium and lead isotopes quite well as discussed in Refs. [3,5,23,36,37]. Figure 4 shows the PES for ^{188,190,192}Po and ^{184,186,188}Pb. In the $^{194-198}$Po isotopes (not shown here) the lowest minimum has a small quadrupole deformation ($|\beta_2| \leqslant 0.1$) reflecting the polarization effect of the valence proton pair. We will further refer to this minimum as the nearly spherical configuration. An oblate (γ =−60°) minimum at $|\beta_2| \sim 0.2$ develops as a shoulder in the PES of ^{198}Po and becomes more pronounced in the lighter isotopes, in ^{192}Po the oblate and nearly spherical configurations are nearly degenerate. One expects a mixed oblate—nearly spherical ground-state configuration, which is confirmed by in-beam and α-decay data [4,24]. In ^{190}Po the oblate minimum is lowest in energy and a prolate (γ=0°) structure with a relatively large prolate deformation ($|\beta_2|$ =0.25) occurs at an excitation energy of only ~170 keV. In a recent in-beam study of ^{190}Po the states from spin $4\hbar$ onwards are attributed to the prolate configuration [37]. In ^{188}Po the prolate minimum at $|\beta_2|$=0.3 becomes lowest in energy for the first time in Po nuclei, while the oblate and spherical configurations rise in energy rapidly compared to the heavier Po isotopes. For the lead isotopes the absolute minimum is at spherical shape, associated with the closed Z=82 shell. The oblate minimum rises in energy going from ^{188}Pb to ^{186}Pb and disappears in ^{184}Pb. A minimum with a large prolate deformation $|\beta_2| \sim 0.3$ appears in ^{186}Pb and becomes more defined and lowers its energy in ^{184}Pb.

The change in the ground-state configuration of polonium and in the composition of the low-lying 0^+ states in lead will influence the α-decay rates. Figure 5 shows the systematics of reduced α-decay widths for the decay to the different 0^+ states in lead nuclei as a function of the neutron number of the mother Po nucleus. In the α decay of $^{198-210}$Po one observes the usual trend (exemplified by the Rn isotopes) of an increase in reduced α-decay width when moving away from

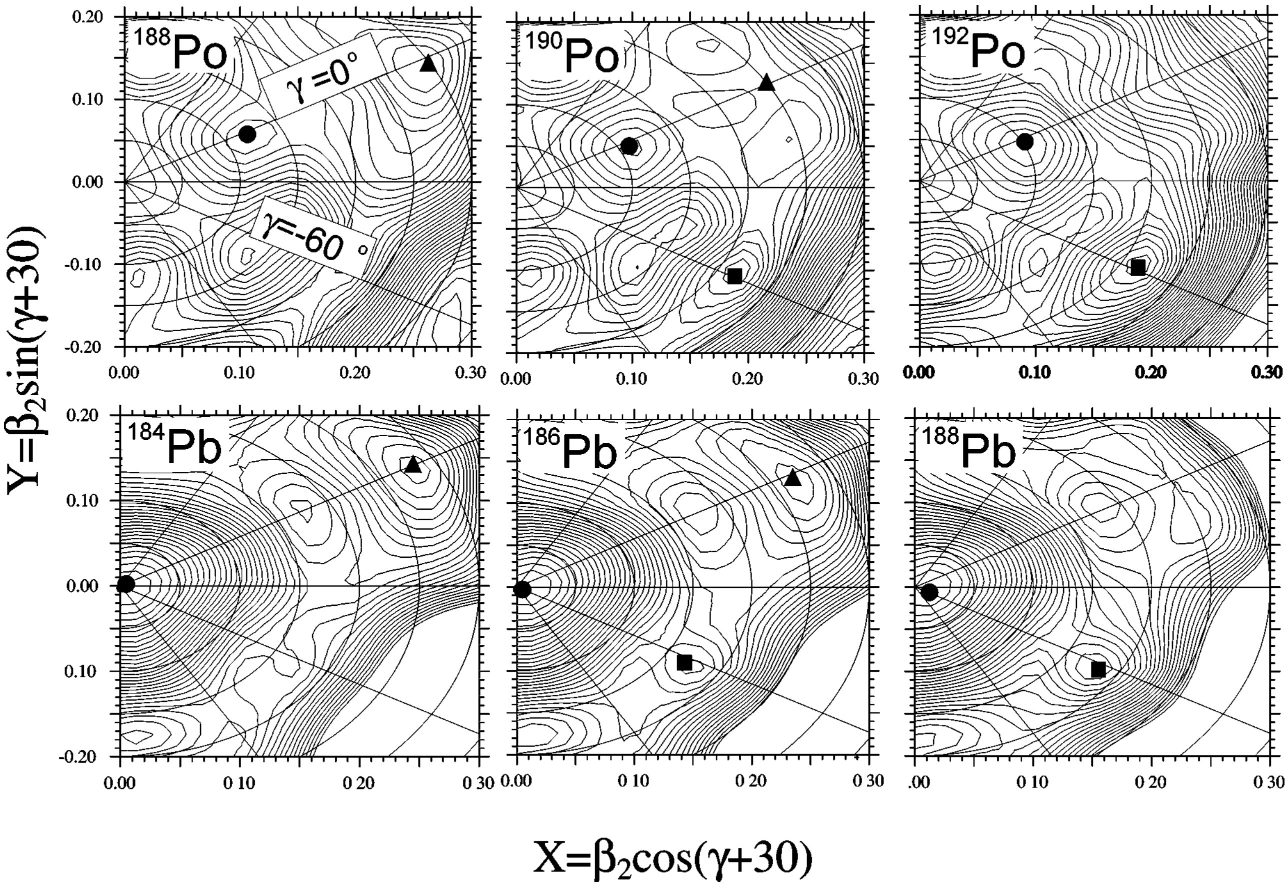

FIG. 4. Potential energy surfaces calculated for ^{188,190,192}Po and ^{184,186,188}Pb. Spherical, oblate, and prolate minima are indicated with circles, squares, and triangles, respectively. The energy separation between the contour lines is 50 keV. The axis of oblate deformation is indicated with $\gamma=-60°$ and of prolate deformation with $\gamma=0°$.

the closed neutron shell at $N=126$. However, for $A\leqslant 198(N\leqslant 114)$ the α-decay strength to the ground state in Pb stays constant and even decreases in ^{188}Po, while the decay to the excited 0^+ state becomes increasingly favored with decreasing neutron number. For $N=108$ (^{192}Po) and below, the reduced α-decay width for the decay to the 0_2^+ state is larger than for the decay to the Pb ground state and the difference between $\delta^2(0^+\rightarrow 0_1^+)$ and $\delta^2(0^+\rightarrow 0_2^+)$ grows when going to $N=104$. By adding up the reduced α-decay width for the decay to the ground state and to the excited state(s) the trend similar to the Rn isotopes is restored.

The observed trend of the reduced widths can be explained using a schematic α-decay model introduced in Ref. [38]. In this model the α decay of the intruder $\pi(4p\text{-}2h)$ or $\pi(6p\text{-}4h)$ components in the Po ground state to the spherical $\pi(0p\text{-}0h)$ configuration in Pb is considered as a multi-step process and hence is retarded. On the other hand the decay to the $\pi(2p\text{-}2h)$ or $\pi(4p\text{-}4h)$ configurations in Pb involves only the removal of a pair of protons from above or below the $Z=82$ shell gap and hence it is given a larger transition probability. The ground state of Pb remains of a rather pure spherical $\pi(0p\text{-}0h)$ nature, the mixing of the $\pi(2p\text{-}2h)$ or $\pi(4p\text{-}4h)$ configuration in the ground state is small [30]. An increasing contribution of the deformed $\pi(4p\text{-}2h)$ (oblate)

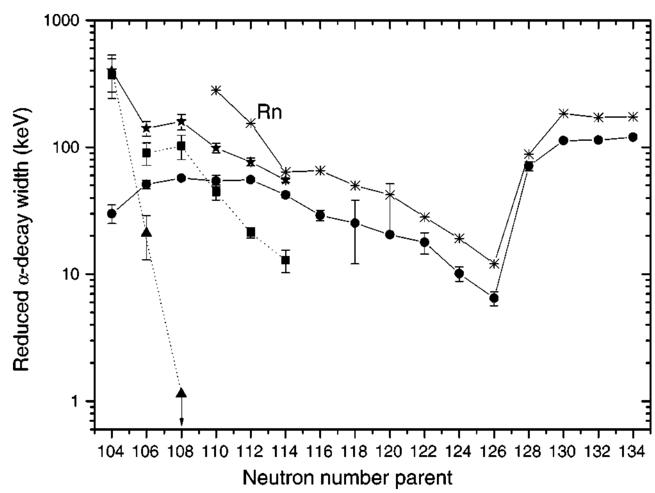

FIG. 5. Reduced α-decay widths as a function of parent neutron number for the decay of Po to the different 0^+ states in the Pb isotopes. The ground-state to ground-state decay of Po is shown with filled circles. The reduced widths for the decay to the presumed oblate and prolate 0^+ states are shown with squares and triangles, respectively. The sum of the values for the different fine-structure α decays is shown with stars. The reduced α-width values for the α decay of Rn are shown with crosses. Lines connect similar configurations to guide the eye. Experimental results are taken from Refs. [5,7,12,31,39] and the present work.

and $\pi(6p\text{-}4h$ or $8p\text{-}6h)$ (prolate) configurations in the ground-state wave function of the light polonium nuclei can explain the retardation observed in the decay to the relative pure Pb ground state and hence the smaller $\delta^2(0^+\rightarrow 0_1^+)$ values as the neutron number decreases towards $N=104$, midshell between 82 and 126. The decay to the deformed excited 0^+ states in lead which contain the $\pi(2p\text{-}2h)$ or $\pi(4p\text{-}4h)$ configuration becomes increasingly favored when moving to the neutron midshell.

Combining this information with the PES results leads us to assign a mainly oblate configuration to the ^{190,192}Po ground states and to the 0_2^+ states in ^{186,188}Pb. A prolate component in the ^{190}Po ground state [37] can be responsible for the decrease in the reduced-width value for the decay to the ^{186}Pb ground state and for the feeding of a third 0^+ state in ^{186}Pb of mainly prolate character [11]. The decay of the mainly prolate ground state of ^{188}Po to the ^{184}Pb ground state is largely retarded, in contrast to the decay to the excited 0^+ state associated with the prolate configuration which is very enhanced.

The change in the reduced α-decay systematics thus indicates that the structure of the Po ground state and of the low-lying 0^+ states in Pb changes as a function of neutron number, the combination with the PES calculations allows one to propose configuration assignments. But clearly the identification of nonyrast (particularly 0^+) states is required to establish the relative positions of the pure oblate and prolate configurations and the interaction strength acting between them to obtain a full picture of the shape coexistence in these nuclei.

V. CONCLUSIONS

We have studied the fine structure in the α decay of ^{192,188}Po at the velocity filter SHIP using an α-particle-electron-γ coincidence measurement setup. More precise values on the decay characteristics to the different 0^+ states in ^{184,188}Pb were measured and conflicting results on a possible 0_3^+ state in ^{188}Pb were clarified. Substantial feeding to excited 0^+ states in ^{184,186,188}Pb, which are of mainly deformed character, indicates that the deformed configurations constitute the main part of the ground-state wave function in ^{188,190,192}Po.

ACKNOWLEDGMENTS

We thank the UNILAC staff for providing the stable and high intensity ^{50,52}Cr beams. This work was supported by the Access to Large Scale Facility program under the Training and Mobility of Researchers program of the European Union within Contract No. HPRI-CT-1999-00001, by the EXOTAG Contract No. HPRI-1999-CT-50017, by the Interuniversity Attraction Poles Program—Belgian State—Federal Office for Scientific, Technical and Cultural Affairs (IAP Grant No. P5/07), and by a Concerted Research Action (Grant No. GOA/99/02, K.U. Leuven). K.V.d.V. is research assistant of the FWO-Vlaanderen. A.N.A. was partially supported by the GREAT Contract No. EPSRC GR/M79981.

[1] K. Heyde *et al.*, Phys. Rep. **102**, 291 (1983).
[2] J. L. Wood *et al.*, Phys. Rep. **215**, 101 (1992).
[3] A. M. Oros *et al.*, Nucl. Phys. **A645**, 107 (1999).
[4] N. Bijnens, Ph.D. thesis, University of Leuven, 1998.
[5] A. N. Andreyev *et al.*, Nature (London) **405**, 430 (2000).
[6] R. Julin *et al.*, J. Phys. G **27**, R109 (2001).
[7] R. B. Firestone, *Table of Isotopes* (Wiley, New York, 1996).
[8] P. Van Duppen and M. Huyse, Hyperfine Interact. **129**, 149 (2000).
[9] J. Heese *et al.*, Phys. Lett. B **302**, 390 (1993).
[10] A. M. Baxter *et al.*, Phys. Rev. C **48**, R2140 (1993).
[11] R. D. Page *et al.*, in *Proceedings of the Third International Conference on Exotic Nuclei and Atomic Masses*, edited by J. Äystö, P. Dendooven, A. Jokinen, and M. Leino (Springer-Verlag, Berlin Heidelberg, 2003), p. 189.
[12] A. N. Andreyev *et al.*, Eur. Phys. J. A **6**, 381 (1999).
[13] N. Bijnens *et al.*, Z. Phys. A **356**, 3 (1996).
[14] R. G. Allatt *et al.*, Phys. Lett. B **437**, 29 (1998).
[15] A. N. Andreyev *et al.*, J. Phys. G **25**, 835 (1999).
[16] Y. Le Coz *et al.*, EPJdirect **A3**, 1 (1999).
[17] G. D. Dracoulis *et al.*, Phys. Rev. C **67**, 051301(R) (2003).
[18] G. Münzenberg *et al.*, Nucl. Instrum. Methods **161**, 65 (1979).
[19] S. Hofmann, Rep. Prog. Phys. **69**, 639 (1998).
[20] J. Wauters *et al.*, Phys. Rev. C **47**, 1447 (1993).
[21] GEANT Detector Simulation Tool, CERN, Geneva, 1993, see http://wwwinfo.cern.ch/pl/GEANT
[22] A. N. Andreyev, http://npg.dl.ac.uk/GREAT/geant_gr.htm
[23] K. Van de Vel *et al.*, Phys. Rev. C **65**, 064301 (2002).
[24] K. Helariutta *et al.*, Eur. Phys. J. A **6**, 289 (1999).
[25] W. Younes *et al.*, Phys. Rev. C **52**, R1723 (1995).
[26] N. Fotiades *et al.*, Phys. Rev. C **55**, 1724 (1997).
[27] K. S. Toth *et al.*, Phys. Rev. C **60**, 011302 (1999).
[28] A. N. Andreyev *et al.* (to be published).
[29] G. L. Poli *et al.*, Phys. Rev. C **63**, 044304 (2001).
[30] P. Dendooven *et al.*, Phys. Lett. B **226**, 27 (1989).
[31] J. Wauters *et al.*, Phys. Rev. C **47**, 1447 (1993).
[32] J. Wauters *et al.*, Phys. Rev. Lett. **72**, 1329 (1994).
[33] P. Van Duppen *et al.*, Ph.D. thesis, University of Leuven, 1985.
[34] J. O. Rasmussen, Phys. Rev. **113**, 1593 (1959).
[35] W. Satula and R. Wyss, Phys. Scr. **T56**, 159 (1995).
[36] A. N. Andreyev *et al.*, Phys. Rev. C **66**, 014313 (2002).
[37] K. Van de Vel *et al.*, Eur. Phys. J. A **17**, 167 (2003).
[38] J. Wauters *et al.*, Phys. Rev. C **50**, 2768 (1994).
[39] H. Kettunen *et al.*, Phys. Rev. C **63**, 044315 (2001).